HYBRID DEM GENERATION AND EVALUATION FROM SPACEBORNE RADARGRAMMETRIC AND OPTICAL STEREOSCOPIC DEMS

C. Xu *, M. Wei, S. Griffiths, B. Mercer, and R. Abdoullaev

Intermap Technologies Corp.
635 6th Ave SW, Calgary, Alberta, T2P 0T5, Canada
(cxu, mwei, sgriffiths, bmercer, rabdoullaev)@intermap.com

Earth Observation for a Changing World

KEY WORDS: Hybrid DEM, Radargrammetric, Photogrammetric, Stereoscopic, Spaceborne, Airborne, Intermap, NEXTMap

ABSTRACT:

With the launch of the recent high-resolution Synthetic Aperture Radar (SAR) satellite missions, e.g., TerraSAR-X, RadarSAT-2, and CosmoSkymed, the technique of radargrammetry motivates interest again to potentially improve upon the level of detail and accuracy of Digital Elevation Models (DEM) from a global coverage perspective as an alternative to data derived from Interferometric SAR (IFSAR), Light Detection and Ranging (LiDAR), or the Shuttle Radar Topography Mission (SRTM). A stereo-radargrammetric DEM extraction capability has been developed in-house with large area operational capacity. A number of DEMs, posted at 10 meters, have been generated from the TerraSAR-X strip-map mode stereo images, and evaluated relative to Intermap's NEXTMap airborne DEM (vertical accuracy specification is 1 meter RMSE for a 5 meter grid). Vertical accuracies of 3~5m (RMSE) were observed in the low-relief, bare terrain areas, which outperformed, in these cases, a 90 m SRTM DEM that had been re-sampled to a 10 meter grid. However, the implementation of the stereo radargrammetry concept has some limitations. For instance, the resulting DEM is severely strongly affected by speckle in the images. Therefore the terrain needs to be overly smoothed and this results in a loss of spatial resolution and accuracy. Although the stereo DEM can be improved with the application of a speckle reducing filter and through development of more efficient image matching algorithms, another approach is through merging with a complementary source, such as a photogrammetrically-derived DEM. The medium-resolution optical stereo images from ALOS/PRISM, are candidates for this approach. However, photogrammetric DEMs also have their intrinsic limitations, for instance, cloud coverage, and in the areas of interest the potential absence of Ground Control Points (GCPs). Without vendor-provided Rational Polynomial Coefficients (RPC), the performance of a 5m posting PRISM stereoscopic DEM from the nadir and backward view combination dramatically depends on the number and quality of input GCPs. Therefore, the fusion of the radar and optically-derived DEMs offers complementary advantages for the creation of a hybrid product. Our preliminary evaluation results show that such a hybrid DEM after fusion does demonstrate superior characteristics in terms of accuracy and level of spatial detail, compared to each individual input. In this work we will outline the process and demonstrate the results visually and quantitatively.

1. INTRODUCTION

Stereo radargrammetry, which is the science of deriving Digital Elevation Model (DEM) using Synthetic Aperture Radar (SAR) stereo image pairs with substantially different incidence angles, has been applied to airborne and subsequently satellite image pairs (particularly RadarSat-1) since the 1980's (Leberl 1990). Its utility lay in mapping large areas, particularly in cloud-obscured areas of the world and in the areas where access by aircraft is not practical. A comprehensive review of the technique is published by Toutin and Gray (2000). With much better satellite positioning information (less than 1m accuracy), the more recent availability of higher resolution imagery (TerraSAR-X, CosmoSkymed, RadarSAT-2 satellite missions) motivates interest again in performing stereo radargrammetry in order to potentially improve upon the level of detail and accuracy. A stereo-radargrammetric DEM is able to provide worldwide coverage via such satellite missions, while airborne platforms are subject to "no-fly" or "no-image" zone restrictions. Such spaceborne imagery based DEM extraction process has been developed in-house at Intermap with the operational capacity for large areas. A number of 10m gridded radargrammetric DEMs, generated from the TerraSAR-X strip-map mode stereo images, have been quantitatively evaluated. Relative to Intermap's high-accuracy NEXTMap airborne interferometric DEM (vertical accuracy specification is 1 meter RMSE for a 5 meter grid), vertical accuracies of 3~5m (RMSE) were observed in the low-relief, bare terrain areas, which outperforms a re-sampled 10m posting SRTM (Shuttle Radar Topography Mission) DEM. However, the implementation of the radargrammetry concept has some limitations, for instance, the DEM is severely affected by noise and speckle in the images. Therefore the terrain needs to be overly smoothed and this results in a loss of spatial resolution and accuracy. Although radargrammetric DEM can be improved with the application of reducing noise level and developing more efficient image matching algorithms, another approach for the improvement is through merging the radargrammetric DEM with a complementary source, such as a photogrammetrically-derived DEM, which mostly employs the mathematical co-linearity model. The proposed fusion of the radar and optically-derived DEMs offers complementary advantages for the creation of a hybrid product.

---

* Corresponding author.

In the paper we demonstrate that such a hybrid DEM does show superior characteristics in terms of accuracy and level of spatial detail, compared to each individual input. In Section 2, the TerraSAR-X mission and the principle of radargrammetric method will be briefly described, and the corresponding stereoscopic DEM is extracted with the illustration of its characteristics. As a complementary approach, the PRISM mission and the photogrammetric method will be addressed in Section 3, and the optical stereo DEM and its characteristics are also discussed. The principle to fuse both radargrammetric and photogrammetric DEMs to generate a superior hybrid DEM will be explained in Section 4. The results are demonstrated visually and quantitatively. In additional, evaluation in both the spatial and spectral domains is discussed.

2. TERRASAR-X RADARGRAMMETRIC DEM

2.1 TerraSAR-X Mission

TerraSAR-X is a German Earth-observation satellite that has been launched and operated since June, 2007. The scheduled lifetime is 5 years. The objective of the mission is to provide value-added SAR data in the X-band and to create new, high-quality radar images of the Earth's surface at an unprecedented level of accuracy (TerraSAR-X website). The satellite flies at a nominal orbital altitude of 514 km with an inclination of 97.44°. The Sun-synchronous orbit has a repeat cycle of 11 days.

The high frequency X-band SAR sensor of TerraSAR-X can be operated in different modes (resolutions) and polarization. It operates three different modes: "Spotlight", "Stripmap", and "ScanSAR". For our purpose of DEM generation, the "Stripmap" model image is used because its resolution meets the requirement of the DEM specification and it is a cost-effective commercial application considering its image coverage (normal footprint 30km x 50km). In addition, the fixed pointing angle of the "Stripmap" mode results in a constant image quality in the azimuth direction. In terms of geometric projection, the Multi-Look Ground Range Detected (MGD) product is used because on the one hand, multi-looking reduces speckle, and on the other hand pixel spacing is equidistant in azimuth and ground range directions which is convenient.

2.2 Radargrammetric Method
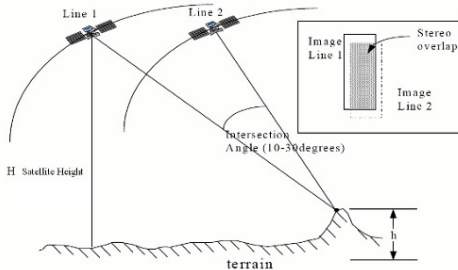
Figure 1. Stereo geometry of radargrammetry (Mercer et al., 1994)

Defined in Leberl (1990), radargrammetry is the technology of extracting geometric object information from radar images. In our work, radargrammetry particularly derives topographic map (DEM) from the disparity angles, which is the angle of parallax, of two overlapping stereo radar images. The two-dimensional geometric representation is portrayed in Figure 1, where the same side looking angle images reduce geometric disparity (Wegmuller et al., 2003).

In radargrammetry, the rigorous extraction of three-dimensional geometric data is defined by a radar stereo intersection. Based on the knowledge of interior orientation (image pixel and line coordinates) as well as exterior orientation (satellite positions and velocities), the solution is represented as the intersection of a range sphere and Doppler cone (Leberl, 1990):

$$\left| \vec{p} - \vec{s} \right| = r , \qquad (1)$$

and,

$$\dot{\vec{s}} \cdot (\vec{p} - \vec{s}) = r \left| \dot{\vec{s}} \right| \sin \gamma , \qquad (2)$$

where
$\vec{p}$ is the unknown vector of the target,
$\vec{s}$ is the vector of satellite position,
$\dot{\vec{s}}$ is the vector of satellite velocity,
r is the slant range of the point and satellite,
and γ is the squint angle.

For TerraSAR-X, the image is processed at the zero Doppler, which means the squint angle $\gamma = 0$. Therefore, Equation (2) can be simplified as:

$$\dot{\vec{s}} \cdot (\vec{p} - \vec{s}) = 0 , \qquad (3)$$

Since a pair of stereo images provides two sets of slant range and satellite ephemeris information, it is an over-determined solution of three unknowns from four range sphere intersection (RSI) equations. Based on stereo geometry, the averaging solution takes the mean value of two vector solutions. The difference between two solutions can be treated as mis-closure, which is an evaluation parameter to quantify the accuracy of the solution.
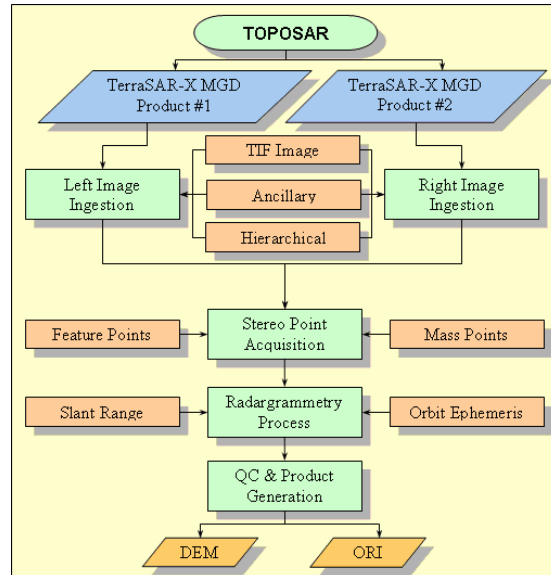
Figure 2. Process flow of TOPOSAR system

2.3 TerraSAR-X DEM Generation and its Characteristics

An Intermap in-house developed software system, referred to as TopoSAR, has been created to generate DEMs radargrammetrically, with large area operational capacity. It is currently hosted on a Linux operating system with a stereo interface. Figure 2 shows the process flow of the end-to-end TopoSAR system. There are basically four major stages: image ingestion of the stereo image pair, stereo point acquisition (manual collection and automated image matching), radargrammetry RSI calculation and coordinate transformation, and residual-based quality control (QC) & DEM product generation.

A number of 10m posted radargrammetric DEMs, generated from the TerraSAR-X strip-map mode stereo images, have been evaluated. Figure 3a shows one DEM example in a moderate terrain relief area, and Figure 3b shows the slope angles in this area of interest (AOI). Intermap's NEXTMap DEM is utilized as the reference for comparison and evaluation of the radargrammetric DEM. Based on the proprietary airborne Interferometric Synthetic Aperture Radar (IFSAR) digital mapping technology, Intermap's NEXTMap DEM essentially is a 3D mapping product created by processing raw radar data collected by airborne IFSAR systems. Height information is obtained in a single-pass mode by using the phase difference between two coherent SAR images, simultaneously obtained by two antennae separated with a constant across-track baseline (Bamler and Hartl, 1998). Li et al. (2004) presented the detailed Intermap IFSAR operation system and production process. According to Intermap's core product specification (Intermap website), the high-quality NEXTMap DEM has a vertical accuracy of 1 m RMSE for a 5 m posting grid (Type I), and provides geospatial professionals worldwide with uniformly accurate wide-area 3D digital elevation data. The high resolution NEXTMap DEM is shown in Figure 4a.
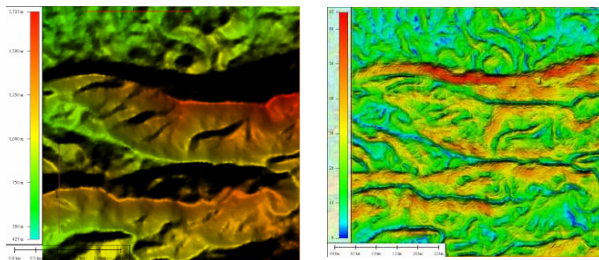
a, TopoSAR DEM   b, Slope angle map
Figure 3. Example of the TopoSAR DEM and slope map
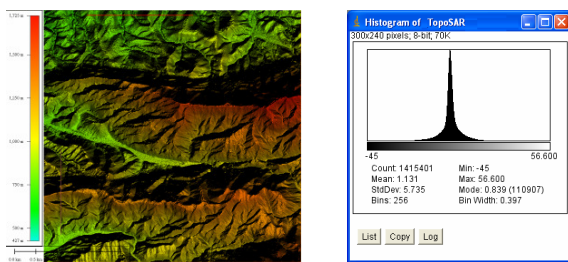
a, NEXTMap DEM   b, Histogram
Figure 4. The reference NEXTMap DEM & difference with TopoSAR histogram

By taking the difference between the TopoSAR DEM and the reference NEXTMap DEM, the histogram and statistical number for the points only below slope angle of 10 degree are listed in Figure 4b, where the mean is 1.1 m, the Standard Deviation (STD) is 5.7 m, and the Root Mean Squared Error (RMSE) can be calculated as 5.8m. Xu et al. (2009) demonstrated that in general a TopoSAR DEM has vertical accuracies of 3~5m (RMSE) in the low-relief bare terrain areas, which outperforms a re-sampled 10m posting SRTM DEM

Two cross section elevation profiles in Figure 5 show that the TopoSAR DEM (in Magenta) follows the similar pattern of the NEXTMap DEM (in Red), but the elevation of the former DEM is much smoother and is missing the peak areas of hills and valleys, compared to the latter one. The reason is that the noise and speckle in the input stereo images result in an in-sufficient point cloud out of the automated image matching.
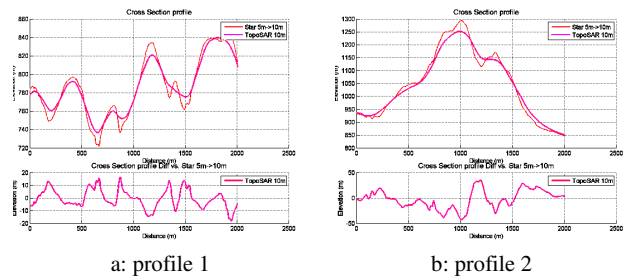
a: profile 1   b: profile 2
Figure 5. DEM comparison and difference of elevation profile

Based on the evaluation of the TopoSAR DEM, the characteristics can be summarized as follows:

1. The TopoSAR DEM shows a homogenous long term feature similar to the NEXTMap DEM;
2. The TopoSAR DEM demonstrates the stable accuracy in the low relief areas with a relatively low noise level;
3. The TopoSAR DEM has overly smoothed hill tops and valleys, and the spatial content needs to be improved. This motivated the interest in merging with a complementary source such as a photogrammetrically-derived DEM.

3. PRISM PHOTOGRAMMETRIC DEM

3.1 PRISM Mission

The Advanced Land Observing Satellite (ALOS) has been developed to contribute to the fields of mapping, precise land coverage observation, disaster monitoring, and resource surveying. The sun synchronous satellite was launched in 2006. The Panchromatic Remote-sensing Instrument for Stereo Mapping (PRISM), a radiometer with 2.5m spatial resolution at nadir, is expected to generate worldwide Digital Maps in respects of its high resolution and stereoscopic observation (ALOS/PRISM website). PRISM has three independent optical systems for viewing nadir, forward and backward producing a stereoscopic image along the satellite's track. Each telescope consists of three mirrors and several CCD detectors for push-broom scanning. The nadir-viewing telescope covers a width of 70 km; forward and backward telescopes cover 35 km each.

3.2 Photogrammetric Method

In principle, the photogrammetric DEM can be extracted based on the collinearity equation, which is a physical model

representing the geometry between a sensor (projection center), the ground coordinates of an object, and the image coordinates:

$$x = -c \frac{R_{11}(X-X_0) + R_{12}(Y-Y_0) + R_{13}(Z-Z_0)}{R_{31}(X-X_0) + R_{32}(Y-Y_0) + R_{33}(Z-Z_0)}$$
$$y = -c \frac{R_{21}(X-X_0) + R_{22}(Y-Y_0) + R_{23}(Z-Z_0)}{R_{31}(X-X_0) + R_{32}(Y-Y_0) + R_{33}(Z-Z_0)} \quad (4)$$

where c is focal length

          x, y are image coordinates

          X_0, Y_0, Z_0 are coordinates of projection center

          X, Y, Z are object coordinates in ground system

          $R_{i,j}$ are the coefficients of the rotation matrix

3.3 PRISM DEM Generation and its Characteristics

Despite three available combinations from three PRISM views, a nadir and backward combination is used to extract the optical DEM because such a combination has the least positioning errors (Saunier 2007). Based on the rigorous 'Toutin Model' (Toutin 2003), the PRISM DEM is extracted using the PCI Geomatica ortho-engine module (PCI Geomatica OrthoEngine Manual). The process flow is demonstrated in Figure 6. Without the vendor provided Rational Polynomial Coefficients (RPC), as was the case in this instance, generating a 5m posting PRISM DEM must rely on the number, distribution and quality of the GCPs (Ground Control Points), In our case, the TopoSAR derived radargrammetric DEM and ORI are utilized as the source of the GCP extraction (Figure 6). If the PRISM DEM fails the acceptance in the QC process, more GCPs with a better distribution will be collected and a new DEM is extracted based on the available updated GCPs. According to the manual, the rigorous Toutin's model requires a minimum of six GCPs. Twelve GCPs were collected for this work to allow the model more redundancies.
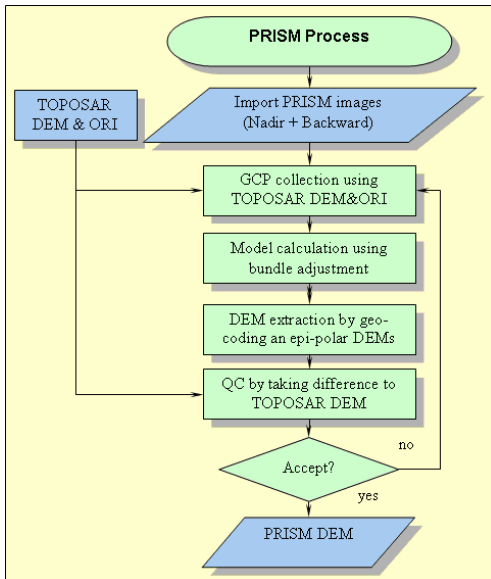
Figure 6. Process flow of PCI ortho-engine DEM extraction

A 5m gridded PRISM DEM was generated based on the process in PCI's ortho-engine described above and is shown in Figure 7a. Intuitively, the PRISM DEM contains more spatial detail than the TopoSAR DEM, but is much noisier on the other hand. The histogram and statistical parameters of the difference surface (PRISM – NEXTMap) are shown in Figure 7b (for slopes <10°), where it shows the mean difference value (PRISM bias) is 47.9 m, STD value is 30.2 m, and the RMSE is 56.6m. With such a large bias number, the accuracy level of the PRISM DEM is much worse than the TopoSAR DEM performance. The large long term drift is mostly caused by the quality, number and distribution of GCPs. In addition, some artificial patterns appear as a result of poor image matching points during DEM extraction.
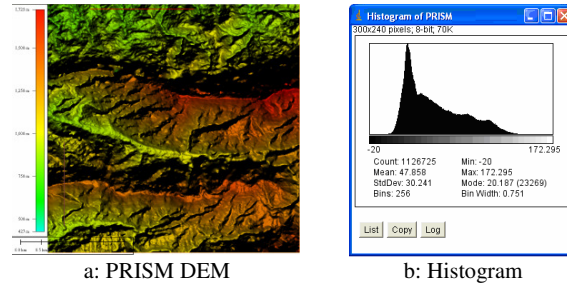
a: PRISM DEM   b: Histogram
Figure 7. The PRISM DEM & difference histogram

Two cross section elevation profiles of the PRISM DEM (in Black) in Figure 8 confirm such a bias in elevation. However, instead of the smoothness of the TopoSAR DEM, the profiles show clearly the PRISM DEM captures most high frequency terrain features, e.g., peaks and valleys.
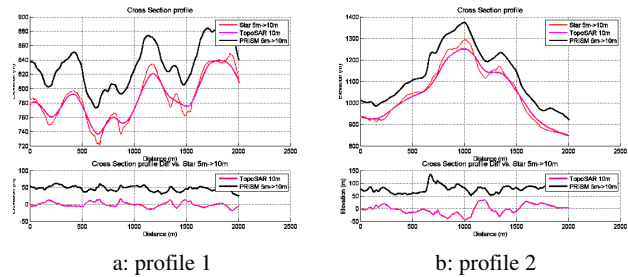
a: profile 1   b: profile 2
Figure 8. DEM comparison and difference of elevation profile

The evaluation of the PRISM DEM shows the following characteristics:
1. The PRISM DEM with a 5 m posting indicates more detailed geospatial contents;
2. The PRISM data exhibits bias or drift errors (possibly due to lack of the knowledge of GCPs or sensor information);
3. The PRISM DEM is noisier with anomalous behaviour, such as spikes or artificial patterns.

4. HYBRID DEM FUSED FROM TERRASAR-X DEM AND PRISM DEM

4.1 Proposed Fusion Method of Hybrid DEM Generation

As analyzed above, the TopoSAR DEM has a robust homogenous long term characteristic but a lower spatial resolution. On the other hand, the PRISM DEM can often

capture the high frequency content but has a lower accuracy due to the bias errors and noise. Thus, a fusion method is proposed and developed based on the principle of adapting the merits of two input DEMs and reducing their individual limitations.

By considering the different characteristics of the TopoSAR DEM and the PRISM DEM, the proposed hybrid DEM process to merge these two products is described in the following steps and also illustrated in Figure 9:

1. Form a difference surface between two input DEMs and remove the areas with outliers in the DEM difference,
2. Estimate the long term discrepancy of the difference surface and adjust accordingly;
3. Apply a smoothing/filtering method to filter the noise of the difference surface while preserving the spatial signal, and then superpose the modified difference onto the PRISM DEM;
4. Generate the hybrid DEM by merging the TopoSAR DEM and the modified PRISM DEM using an optimal weighting model based on the slope information from the TopoSAR DEM.
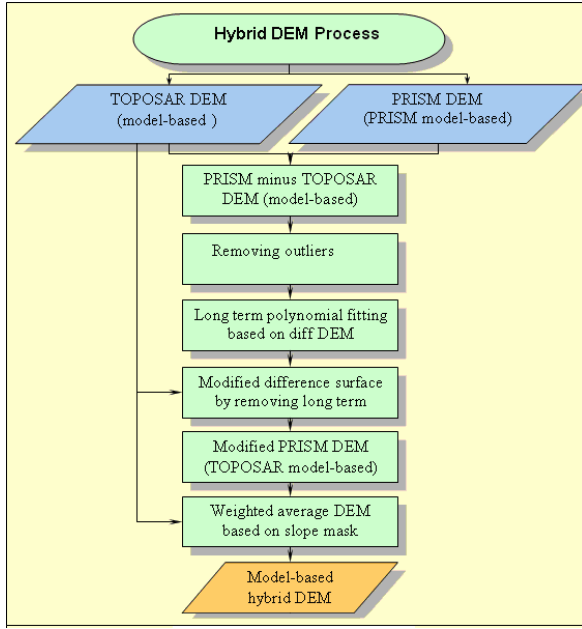
Figure 9. Process flow of the proposed hybrid DEM generation

4.2 Evaluation of Hybrid DEM

A 10m posting hybrid DEM based on the proposed fusion method was generated by merging the TopoSAR DEM and the modified PRISM DEM. The accuracy evaluation is performed in both spatial domain (Figure 10 and Figure 11) and spectral domain (Figure 12).

4.2.1 Spatial Evaluation
The statistical accuracy of three DEMs, compared to the NEXTMap reference data, is summarized in Table 1 (Units are meters). For the hybrid DEM (Figure 10a), the mean value is 1.7m and STD is 5.1m, which leads to a RMSE value of 5.4m. It reserves the long term accuracy from the TopoSAR DEM and the RMSE accuracy is slightly better than the TopoSAR DEM.
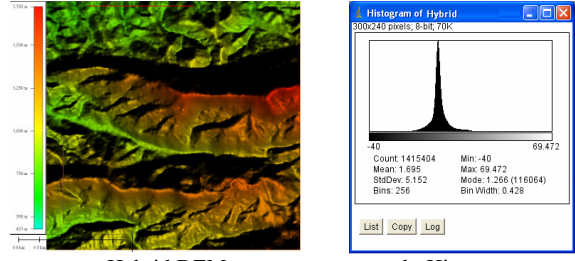
a: Hybrid DEM   b: Histogram
Figure 10. The hybrid DEM & difference histogram

Table 1. Accuracy assessment relative to the NEXTMap reference DEM

	Mean	STD	RMSE
TopoSAR DEM	1.1	5.7	5.8
PRISM DEM	47.9	30.2	56.6
Hybrid DEM	1.7	5.1	5.4

Two cross section elevation profiles in Figure 11 show that the local features in the hybrid DEM (in Blue), which the PRISM DEM contains, are captured and they are now much closer to the NEXTMap reference spatial content.
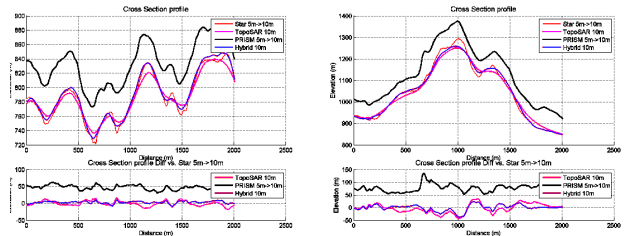
a: profile 1   b: profile 2
Figure 11. DEM comparison and difference of elevation profile

4.2.2 Spectral Evaluation
A spectral analysis is also performed on the individual DEMs. The auto-correlation $R(\tau)$ at a spacing of τ is an efficient model for correlated observations in the spatial domain. Its Fourier transform can be represented as Power Spectral Density (PSD), $S(f)$, in the frequency domain, which describes how the power of a signal or a noise is distributed with frequency.

$$S(f) = \int_{-\infty}^{\infty} R(\tau)e^{-j2\pi f\tau}d\tau \tag{5}$$

where f is the frequency.

The centralized 2D power spectral density of different DEMs is plotted in Figure 12. The brighter the PSD profile, the more spatial content is found in the spectral image. The extent of the frequency components represented in these plots also provides an indication of spatial content. For example, Compared to the SRTM resampled 10m posted DEM, the TopoSAR PSD plot shows a significant power in the center low frequency areas but typically insignificant but still a better power in the corners of

the plot area with high frequencies. Meanwhile, the PRISM PSD shows a relatively much brighter pattern indicating a richer spatial content, but it has some heterogeneous artifacts in the high frequency areas. As a merged result, the hybrid DEM PSD has a moderate and homogeneous power over the frequency.
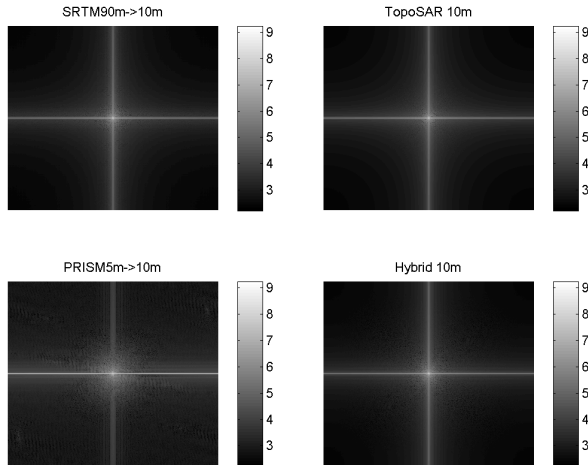
Figure 12. Two-dimensional PSD analysis

The evaluation in both spatial and spectral domain shows that the major advantages of the hybrid DEM, compared to each individual input DEM, are as follows:

1. The hybrid DEM reserves the long term terrain with a slightly better accuracy level to the TopoSAR DEM;
2. The hybrid DEM inherits the high frequency spatial features from the PRISM DEM.

5. CONCLUSION

Intermap has developed the TopoSAR system, an in-house stereo-radargrammetric process, to generate DEMs from spaceborne SAR imagery. Although it has a consistent average behaviour compared to the reference NEXTMap data, the typical 10m gridded TopoSAR DEM smoothes out the high frequency spatial signal. As a complementary optical source, a PRISM sensor based photogrammetric DEM is generated using PCI's OrthoEngine module from a nadir + backward combination. This captures most terrain features, but it exhibits large vertical biases which may be caused by the insufficient or inadequately distributed GCP measurements in the absence of vendor-provided RPCs. A fusion process to merge these two individual DEMs was developed to preserve the advantages of each input, thus creating a hybrid DEM with better performance than either individually. The evaluation of the hybrid DEM are conducted in both spatial and spectral domain, and the results of the hybrid DEM demonstrate superior characteristics in terms of accuracy and level of spatial contents, compared to each individual input. Although the fusion algorithm was designed particularly for radargrammetric TerraSAR-X DEM and photogrammetric ALOS/PRISM DEM, it can be applied extensively to a more generic DEM fusion process from two different input DEMs with different characteristics.

Reference

ALOS/PRISM website. ALOS@EORC Home. URL: http://www.eorc.jaxa.jp/ALOS/en/about/prism.htm [Last accessed: 28 April 2010].

Bamler R. and P. Hartl (1998). Synthetic aperture radar interferometry. *Inverse Problems*. Vol. 14: pp. R1-R54.

Intermap website. Intermap Technologies: Digital Mapping. URL: http://www.intermap.com/ [Last accessed: 28 April 2010].

Leberl F. W. (1990). Radargrammetric image processing. Artech House. ISBN: 0-89006-273-0. 595p.

Li X., K. Tennant, and G. Lawrence (2004). Three-dimensional mapping with airborne IFSAR based STAR technology – Intermap experiences. *Proceedings, XX ISPRS Congress*, 12-23 July, Istanbul, Turkey.

Lumsdon P., C. Xu, J. Hou, and J. B. Mercer (2008). Evaluation of digital elevation models from stereo radargrammetry data. *Proceedings, 7th European Conference on Synthetic Aperture Radar*, 2-5 June, Friedrichshafen, Germany. pp. 277–280.

Mercer J. B., S. Griffiths, and S. Thornton (1994). Large area topographic mapping using stereo SAR. *Proceedings, First International Airborne Remote Sensing Conference and Exhibition*, Strasbourg, France. pp. 260-280.

Mercer J. B., S. Thornton, and K. Tennant (1998). Operational DEM production from airborne interferometry and from RadarSAT stereo technologies. *Proceedings, ASPRS – RTI Annual Conference*, March 31 – April 3, 1998, Fampa, Florida, USA. pp. 1-11.

PCI Geomatica OrthoEngine Manual, Version 10.0, URL: http://www.pcigeomatics.com/ [Last accessed: 28 April 2010]

Saunier S. (2007). Final calibration/validation report – PRISM. *GAEL Consultant*, Report Reference #GAEL-P237-DOC-007.

TerraSAR-X website. DLR Portal – TerraSAR-X. URL: http://www.dlr.de/en/desktopdefault.aspx/tabid-4219/ [Last accessed: 28 April 2010].

Toutin T. (2003). Error tracking in Ikonos geometric processing using a 3D parametric model. *Photogrammetric Engineering & Remote Sensing*, Vol. 69(1): pp. 43-51.

Toutin T. and L. Gray (2000). State-of-art of elevation extraction from satellite SAR data. *ISPRS Journal of Photogrammetry and Remote Sensing*, Vol. 55(1): pp. 13-33.

Wegmuller U.; C. Werner; A. Wiesmann, A.; T. Strozzi (2003). Radargrammetry and space triangulation for DEM generation and image ortho-rectification. *Proceedings, IEEE International Geoscience and Remote Sensing Symposium (IGARSS)*, 21-25 July, Toulouse, France. pp. 179-181.

Xu C., S. Griffiths, P. Lumsdon, B. Mercer, and Q. Zhang (2009). Creation and Evaluation of DEMs from TerraSAR-X Stereo Images. *Proceedings, 30th Canadian Symposium on Remote Sensing*, 22-25 June, 2009, Lethbridge, Canada.